

This discussion paper is/has been under review for the journal Atmospheric Measurement Techniques (AMT). Please refer to the corresponding final paper in AMT if available.

# Potential of airborne lidar measurements for cirrus cloud studies

S. Groß<sup>1</sup>, M. Wirth<sup>1</sup>, A. Schäfler<sup>1</sup>, A. Fix<sup>1</sup>, S. Kaufmann<sup>1,2</sup>, and C. Voigt<sup>1,2</sup>

<sup>1</sup>Institut für Physik der Atmosphäre, Deutsches Zentrum für Luft- und Raumfahrt (DLR), Oberpfaffenhofen, 82234 Wessling, Germany

<sup>2</sup>Johannes-Gutenberg-Universität Mainz, Institut für Physik der Atmosphäre, 55122 Mainz, Germany

Received: 17 February 2014 – Accepted: 26 March 2014 – Published: 16 April 2014

Correspondence to: S. Groß (silke.gross@dlr.de)

Published by Copernicus Publications on behalf of the European Geosciences Union.

## Potential of airborne lidar measurements for cirrus cloud studies

S. Groß et al.

Title Page

Abstract

Introduction

Conclusions

References

Tables

Figures

⏪

⏩

◀

▶

Back

Close

Full Screen / Esc

Printer-friendly Version

Interactive Discussion



## Potential of airborne lidar measurements for cirrus cloud studies

S. Groß et al.

Title Page

Abstract

Introduction

Conclusions

References

Tables

Figures



Back

Close

Full Screen / Esc

Printer-friendly Version

Interactive Discussion



e.g. ice crystal shape, size distribution and number concentration (Stephens, 1990; Haag and Kärcher, 2004; Fusina et al., 2007), which are influenced by ambient conditions, especially dynamics (Kärcher and Lohmann, 2003), temperature and super-saturation (Heymsfield, 1977; Khvorostyanov and Sassen, 1998b) as well as the nucleation mode, i.e. the composition of the ambient aerosol (e.g. Ström and Ohlsson, 1998; Seifert et al., 2004). Furthermore, small-scale turbulence is important for the fine structure of cirrus clouds, which affects the inhomogeneity of microphysical properties (Gu and Liou, 2000) and therewith of the cirrus' radiative effect (Liou, 1972). The inhomogeneous nature of cirrus on different spatial scales is one major issue which complicates modelling of their radiative properties. Model simulations usually use idealized cloud structure and microphysics, as well as radiative transfer approximations. To improve the representation of cirrus clouds in simulations and circulation models, we need a better understanding of the micro- and macro-physical properties of cirrus clouds, as well as of small-scale processes within cirrus.

Airborne Differential Absorption Lidar (DIAL) measurements of water vapour (Ehret et al., 1993; Bösenberg, 1998; Browell et al., 1998) provide two-dimensional information of the atmospheric structure, and are thus a suitable tool to study the fine-structure of cirrus clouds, as well as their macro-physical properties. The combination of DIAL water vapour measurements with additional temperature information (e.g. from model analyses or dropsondes) further enables to investigate the variability of relative humidity and ice super-saturation within cirrus clouds which are crucial properties for cirrus cloud evolution (e.g. Heymsfield and Miloshevich, 1995). However, up to now, the high signal dynamics within clouds limited the use of airborne downward looking DIAL measurements for mid-latitude cirrus clouds. An optimal distance of about 2 km to the cirrus cloud is required to avoid an overload of detectors and data acquisition due to the immense signal dynamics in the near field resulting from the  $r$ -dependence of the backscatter signal. Up to now the required flight altitude to examine mid-latitude cirrus clouds up to about 13 km height was only accessible with high altitude aircraft like the Russian stratospheric aircraft Geophysica (Stefanutti et al., 1999) and the NASA

ER-2. With the new German research aircraft HALO (High Altitude and LOng range) (Krautstrunk and Giez, 2012) it is possible to reach flight altitudes of up to 15 km, and thus a sufficient distance to the cirrus cloud top in most cases.

For the first time, measurements of the airborne aerosol and water vapour DIAL WALES (Water vapour Lidar Experiment in Space; Wirth et al., 2009), operated on-board HALO during its first scientific mission (Techno-Mission) are presented. The HALO Techno-Mission took place in October and November 2010 and provided the opportunity to investigate cloud properties with two different aircraft. HALO, flying at a cruise altitude of  $\sim 14$  km probed the cloud ( $\sim 1$  km below cruise altitude) with the lidar. Additionally, the DLR research aircraft Falcon was equipped with in-situ instruments to measure temperature and water vapour mixing ratio within cirrus clouds. This unique combination of these two aircraft provided the opportunity to compare the different measurement strategies, i.e. in-situ and remote sensing measurements with a focus on cirrus cloud studies. Relative humidity with respect to ice (RHi) is determined within the cirrus clouds based on the novel high-altitude DIAL observations combined with ECMWF model analysis temperature data.

Section 2 gives an overview over the aircraft and mission design, the WALES system, and the WARAN in-situ hygrometer on-board the Falcon used for water vapour inter-comparison. Section 3 demonstrates the potential of the DIAL system for cirrus cloud studies based on a case study with measurements inside the cirrus cloud. Section 4 provides a summary and discussion of the main findings. Section 5 gives an outlook to future cirrus cloud observations with remote sensing instruments on-board HALO.

## 2 Data and methods

### 2.1 HALO and Techno-Mission

HALO (Fig. 1) is a modified Gulfstream G550 business jet operated by the flight department of DLR in Oberpfaffenhofen. With a range of more than 8000 km and an

## Potential of airborne lidar measurements for cirrus cloud studies

S. Groß et al.

Title Page

Abstract

Introduction

Conclusions

References

Tables

Figures

⏪

⏩

◀

▶

Back

Close

Full Screen / Esc

Printer-friendly Version

Interactive Discussion



endurance of up to more than 10 flight hours even large scale atmospheric features can be investigated at almost all regions around the globe. A maximum cruising altitude of more than 15 km enables measurements in the upper troposphere and lower stratosphere in high- and mid-latitude regions. With a payload of up to three tons, HALO provides enough capacity to accommodate a synergetic payload to collect a comprehensive atmospheric data set (Krautstrunk and Giez, 2012). Technical details can be found in Table 1.

In the course of the first scientific HALO mission, the so-called Techno-Mission, five flights with HALO aircraft were performed from 28 October to 5 November 2010 out of Oberpfaffenhofen, Germany. The major part of the flights took place in the Temporary Reserved Airspaces (TRA, i.e. military areas with restricted access to commercial aircraft) Allgäu in Southern Germany and Mecklenburg-Vorpommern in North-Eastern Germany (28 October to 29 October and 5 November 2010). Here we present data of the flights on 3 November (from 09:51 to 13:17 UTC) and 4 November (10:21 to 13:32 UTC), 2010. Lidar observations were only possible inside the TRA areas. The 4 November flight data between 10:47 and 11:54 UTC are used for the comparison of remote sensing (lidar) data and in-situ data of the beneath flying Falcon. The measurement situation was characterized by a stationary cirrus cloud covering the whole measurement area. Data from 3 November (10:15 to 11:25 UTC) are used to compare the RHi statistics in a different cloud regime characterized by a transient cirrus cloud drifting out of the measurement area. This gave us the opportunity to perform measurements in cloudy and in cloud free air masses. HALO was equipped with a spectrometer system operated by University of Leipzig together with an instrument for measuring the actinic flux in cooperation with Forschungszentrum Jülich (HALO-SR) (Fricke et al., 2013), an automated high volume air sampling system (MIRAH – Measurements of Stable Isotope Ratios in Atmospheric Trace Gases on HALO) of University of Wuppertal (Krebsbach et al., 2013), and an ion trap mass spectrometer of DLR (Roiger et al., 2011). Additionally, and in the focus of this paper, the DIAL system WALES (Wirth et al., 2009) was provided by DLR Institute of Atmospheric Physics (IPA). The

## Potential of airborne lidar measurements for cirrus cloud studies

S. Groß et al.

Title Page

Abstract

Introduction

Conclusions

References

Tables

Figures



Back

Close

Full Screen / Esc

Printer-friendly Version

Interactive Discussion







2014). The measurement cell is passively flown through using a heated Rosemount inlet system in order to avoid particles, especially ice crystals, entering the inlet line. However, the efficiency of the particle separation is not perfect in some cases so that in-cloud measurements may partly be influenced by evaporating particles.

## 3 Results

### 3.1 Overview

At the time of the observation (12:00 UTC) on 4 November 2010, the synoptic situation over Europe was characterized by a large scale ridge. Cirrus clouds at upper levels were advected towards Germany within the anticyclonic Jetstream (see increased values of relative humidity at 250 hPa in Fig. 2a). Figure 2b shows the flight track of HALO between 10:21 and 13:32 UTC in the TRA Allgäu in Southern Germany. In the following we only consider data from the 910 km long section of the flight between 10:47 and 11:54 UTC (solid line) when measurements were performed at constant flight level of about 14 km. After 11:54 UTC HALO started to descend.

Figure 3a presents the lidar backscatter ratio cross-section at 532 nm, the ECMWF cloud water content, and the flight altitude of the Falcon within the cirrus cloud. The backscatter ratio indicates the cirrus cloud with a base altitude at about 10 km and the cirrus cloud top at about 13 km. The backscatter ratio within the cirrus cloud shows a wide range of values from about 4 up to more than 50. The comparison of the backscatter ratio and the ECMWF cloud ice water content ensures that model data and observation of cloud height and location are in good agreement, a crucial requirement to combine model data and lidar measurements. The Falcon flight track reaches the cloud at constant height level at about 11 km at 11:25 UTC and both aircraft flew in short horizontal distance until 11:54 UTC. Therefore Falcon in-situ measurements during that period can be used for validation of the lidar measurements and comparisons of model data within the cloud. Figure 3b shows the lidar derived upper level (9–13 km)

## Potential of airborne lidar measurements for cirrus cloud studies

S. Groß et al.

Title Page

Abstract

Introduction

Conclusions

References

Tables

Figures

⏪

⏩

◀

▶

Back

Close

Full Screen / Esc

Printer-friendly Version

Interactive Discussion



optical depth (OD) at 532 nm, which is a measure of the attenuation of light on its way through the atmosphere. The OD in the upper level ranges between about 0.1 and 1.5 with a very variable structure.

Figure 4a shows water vapour in-situ measurements from the WARAN on-board the Falcon and remote sensing observations at the same altitude and location by the DIAL WALES. In Fig. 4b the horizontal distance between HALO and Falcon is plotted. The blue line (Fig. 4a and b) indicates the time when the Falcon reached a constant flight altitude of about 10.8 km. Both measurements agree well when the distance between both measurements is less than 10 km (after ~ 11:20 UTC). The mixing ratio during the selected time period is about 100 ppmv. Even small scale features can be resolved well by the WALES-DIAL measurement.

### 3.2 Relative importance of temperature and humidity for the determination of RHi

Additionally to the water vapour measurements the calculation of RHi requires collocated temperature information. As there was no remote measurement of the temperature field beneath HALO 3-dimensional temperature fields provided by ECMWF model are interpolated in space and time to match with the position of the WALES measurement (Schäfler et al., 2010).

To estimate the accuracy of the ECMWF model temperature inside cirrus clouds and its applicability for RHi studies we compare the ECMWF temperature data with in-situ temperature measurements of the Falcon flying in the cirrus cloud beneath HALO. For this purpose, a flight path in which the Falcon flight level of about 10.8 km varied by less than 100 m (11:25–11:54 UTC) was chosen, to avoid uncertainties resulting from sharp vertical temperature gradients at changing flight altitudes.

Figure 5 presents the comparison of the Falcon in-situ measurements and the ECMWF temperature (Fig. 5a), water vapour mixing ratio (Fig. 5b) and derived relative humidity (Fig. 5c). The ECMWF temperature is almost constantly colder than the in-situ measurements with mean values of ~ 219.1 K from ECMWF model analysis

## Potential of airborne lidar measurements for cirrus cloud studies

S. Groß et al.

Title Page

Abstract

Introduction

Conclusions

References

Tables

Figures



Back

Close

Full Screen / Esc

Printer-friendly Version

Interactive Discussion



## Potential of airborne lidar measurements for cirrus cloud studies

S. Groß et al.

Title Page

Abstract

Introduction

Conclusions

References

Tables

Figures

◀

▶

◀

▶

Back

Close

Full Screen / Esc

Printer-friendly Version

Interactive Discussion



and  $\sim 220.0$  K from Falcon in-situ measurements. The mean temperature difference between Falcon measurement and ECMWF in the considered height level is about  $-0.9$  K. The mean value of the water vapour mixing ratio (Fig. 5b) agrees well in the considered time series with mean values of  $\sim 100$  ppmv from model analysis and  $\sim 99$  ppmv from WARAN in-situ measurements, whereas the calculated relative humidity (Fig. 5c) differs by about 11 % ( $\sim 103$  % using ECMWF data and  $\sim 91$  % using in-situ observations of temperature and water vapour) due to a bias in temperature data (Table 3). Additionally, RHi is calculated with WARAN water vapour measurements and ECMWF model temperatures, showing higher RHi values (Fig. 5c) which is due to the lower modelled temperatures. Figure 5 further shows that the local variability of the relative humidity is mainly caused by fluctuations in the water vapour mixing ratio. The smaller temperature fluctuations have a minor influence on RHi within the observed cirrus cloud.

This is also visible regarding the relative variability, which is the ratio of the standard deviation and the mean, of the temperature, the water vapour mixing ratio, and the RHi data within the considered time period. The relative variability of both temperature data sets is similar. In contrast, the distributions of mixing ratio and RHi differ significantly between model analysis and in-situ measurements. The relative variability of mixing ratio and RHi are considerably larger than for the temperature, and differ by factor of around 4 with ECMWF showing less variation than in-situ data. The relative variability of the individual variables is listed in Table 3.

The influence of temperature variability on the variability of relative humidity over ice is further estimated along the Falcon flight section (see Fig. 5) by comparing RHi values calculated with the mixing ratio from WARAN and different temperatures. The relative variability of relative humidity calculated with the Falcon temperature measurements is 0.12, with the uncorrected temperature from ECMWF analysis is 0.13, and with a constant temperature value (i.e. the mean of the Falcon measurements) is 0.12. Values differ only by about 10 % meaning that the major part of local RHi fluctuations is caused by local variations in the water vapour mixing ratio. Temperature variations give only a minor local contribution.

It is worthwhile mentioning that the ECMWF model predicts the cloud where it is detected by lidar. However, additional uncertainties in the absolute values of RH<sub>i</sub> resulting from differences in model temperature and actual temperature have to be taken into account.

### 3.3 Relative humidity over ice within cirrus cloud

To derive RH<sub>i</sub> using WALES water vapour measurements, ECMWF temperature data were interpolated in space and time to match with the measured field. Figure 5 showed differences between observed and modelled temperatures at the flight altitude of the Falcon. To verify the applicability of the model temperature in this altitude range, we compare the vertical profile of different measurements; radiosonde data from the 12:00 UTC ascends over Munich and Stuttgart, ECMWF temperature analysis data at 12:00 UTC, and HALO and Falcon profiles derived from the total air temperature sensors of both aircraft during descent to Oberpfaffenhofen airport (11:57 to 13:32 UTC for HALO and 12:13 to 13:29 UTC for the Falcon) which is closest in time (Fig. 6).

As can readily be seen from Fig. 6a, the temperature profiles of the two radiosonde temperature profiles of Munich and Stuttgart agree well (with minor deviations between 12 and 13 km, i.e. the tropopause region) which indicates little horizontal variability of the temperature field. This is also confirmed by horizontal sections of ECMWF temperature at 10 km altitude (not shown). This is important as the location of the aircraft measurements lies in between both stations. Another important result of this comparison is that the tropopause region between 12 and 13 km altitude is captured well in the model data, confirming that model data are appropriate to use in this altitude range. Also, the temperature profiles from the two aircraft show very comparable results up to the maximum ceiling altitude of the Falcon which is not surprising since both aircraft use the same type of total air temperature sensors (Stickney et al., 1994).

However, differences between the model temperature profile and the temperature profile measured on-board the aircraft descents can be seen (Fig. 6b). Between 9 and 11 km altitude, model and HALO temperature differ nearly height-independent by

## Potential of airborne lidar measurements for cirrus cloud studies

S. Groß et al.

Title Page

Abstract

Introduction

Conclusions

References

Tables

Figures



Back

Close

Full Screen / Esc

Printer-friendly Version

Interactive Discussion



## Potential of airborne lidar measurements for cirrus cloud studies

S. Groß et al.

Title Page

Abstract

Introduction

Conclusions

References

Tables

Figures

⏪

⏩

◀

▶

Back

Close

Full Screen / Esc

Printer-friendly Version

Interactive Discussion

about 0.8 K ( $T_{\text{HALO}} - T_{\text{ECMWF}}$ ), whereas in the upper cloud region (11–13 km altitude) the difference is height dependent and varies between  $-1.4$  K (uppermost level) and about 1.5 K (about 12.2 km). The mean difference in this height range is about 0.6 K. In the entire altitude range (9–13 km) the mean difference is about 0.8 K. The sources of the differences between model and HALO temperature are not entirely clear, although up to altitudes where both radiosondes agree very well ( $\sim 12$  km) the deviation is still within the combined error that is given in the literature ( $\sim 0.3$  K for radiosondes at daytime (Nash et al., 2010) and  $\sim 0.5$  K for the aircraft temperature sensors (Giez, personal communication 2014; Stickney et al., 1994)). Possible reasons may be uncertainties in the temperature measurements of the aircraft due to insufficient correction for flight performance parameters (Giez, personal communication 2014), due to radiation or clouds effects (Nash et al., 2010), or due to resolution artefacts. Comparing radiosonde temperature measurements to model and airborne temperature data we see that model and radiosondes occasionally show good agreements while airborne and radiosonde temperature measurements show similar differences than model and airborne data. To create the analysis fields, preferably the most realistic representation of the state of the atmosphere, ECMWF assimilates multitude of different observation types, e.g. from surface stations, satellites and also radiosondes. This can explain the smaller deviations between modelled temperatures and the radiosonde profiles and may also impact the deviations between model and aircraft data.

Although the uncertainties of the temperature measurements lead to a relative uncertainty of about 10–15% in the retrieved RH<sub>i</sub> in the considered temperature range, we conclude that the ECMWF model temperature field is suited for this kind of study.

In our case we used the available observed temperature profile of HALO to offset the ECMWF temperature field with a vertically constant temperature bias (of 0.8 K) in the altitude range between 10 and 13 km. For the calculation of RH<sub>i</sub> (from WALES and ECMWF data), the Goff Gratch formula (Goff and Gratch, 1946) was used to determine the saturation pressure over ice. The cross section of water vapour mixing ratio (in combination with the model temperature field) and relative humidity over ice



of backscatter ratio and relative humidity over ice for both cirrus regimes. In the persistent cirrus cloud on 4 November 2010 (Fig. 10a) only very few RHi values exceed 120 %; even outside the cirrus at low backscatter ratios. In contrast, in the transient cirrus case (Fig. 10b) high RHi values up to 150 % are found outside the cirrus cloud.

5 In both cases, the corresponding RHi value of the maximum backscatter ratio is about 100 %.

## 4 Summary and discussion

We used combined airborne water vapour lidar measurements and ECMWF temperature data to analyse RHi within a cirrus cloud observed on 4 November 2010. For this analysis it is important that the model is able to reproduce the general cloud situation as otherwise uncertainties may occur mainly due to temperature differences. For the examined case, on 4 November 2010, we therefore verified that the model is able to reproduce the cloud situation in terms of location and vertical extent of the cirrus cloud. This ensures comparability of observed and modelled cloud properties.

15 Considering RHi within the cirrus cloud, we experimentally found that about 30 % of all data points showed supersaturation; but only 2 % of all data points showed higher values than 120 %. This is in good agreement with former findings of about 30 % ice supersaturation within mid-latitude cirrus clouds over the Southern Great Plains from combined Raman lidar measurements (Comstock et al., 2004) and from in-situ measurements in the vicinity of Ireland (Ovarlez et al., 2002) during INCA (INter hemi-  
20 spheric difference in Cirrus properties from Anthropogenic emissions), respectively. The small differences in the observed fraction of supersaturated data points may be explained by an absolute error of about 10–15 % in the RHi data, resulting mainly from uncertainties in the used temperature, as well as from differences of the evolution  
25 stage of the examined cirrus cloud regimes. Considering the INCA dataset, Ovarlez et al. (2002) found that two types of distributions can be fitted to the observations; a Gaussian distribution for warm cirrus clouds ( $T > -40^{\circ}\text{C}$ ), and a Rayleigh distribution

## Potential of airborne lidar measurements for cirrus cloud studies

S. Groß et al.

Title Page

Abstract

Introduction

Conclusions

References

Tables

Figures

◀

▶

◀

▶

Back

Close

Full Screen / Esc

Printer-friendly Version

Interactive Discussion





assume the observed cloud of 4 November 2010 to be in equilibrium with a tendency to dissolve, this may explain the differences in the observed vertical RHi structure.

By comparing the relative humidity inside and outside the cirrus cloud for the fully developed stage on 4 November 2010 we found a limit of RHi values of about 120% inside as well as outside the cloud. This supports the assumption that the cloud is rather stable, maybe with a tendency to evaporate at that stage. High RHi values of approximately 140–150% RHi are needed for homogeneous ice nucleation (DeMott et al., 1998; Koop et al., 2000; Haag et al., 2003; Kärcher 2012). Thus the high RHi values of up to 150% following the transient cirrus cloud on 3 November 2010 suggest that homogeneous ice nucleation may play a role in cirrus cloud formation in this situation. The relative humidity corresponding to the maximum backscatter ratio was ~ 100% in both cases. We interpret that in the centre of the cirrus, where particle density causes high backscatter ratios, the water uptake by and evaporation of ice crystals is in equilibrium. As expected, in both cases the RHi range is much wider outside the cirrus than within.

The presented novel analysis technique enables to classify the evolution stage in the life cycle of the cirrus cloud as it provides information of the RHi distribution shape within the cirrus cloud, the vertical structure of the RHi, and the joint distribution of in-cloud and out of cloud RHi values. As these parameters are (amongst others) dependent on the life cycle of the cloud, the novel analysis technique can give indications whether the cloud is in a formation or dissipation stage. However, additional observations of different cloud regimes and environmental conditions are required for a thorough analysis.

## 5 Conclusion

WALES measurements during the HALO Techno-Mission show the great potential of observing water vapour with a DIAL on board the high altitude aircraft HALO for cirrus cloud studies. The extended vertical range of the HALO aircraft makes it possible to

## Potential of airborne lidar measurements for cirrus cloud studies

S. Groß et al.

Title Page

Abstract

Introduction

Conclusions

References

Tables

Figures

⏪

⏩

◀

▶

Back

Close

Full Screen / Esc

Printer-friendly Version

Interactive Discussion



## Potential of airborne lidar measurements for cirrus cloud studies

S. Groß et al.

Title Page

Abstract

Introduction

Conclusions

References

Tables

Figures

◀

▶

◀

▶

Back

Close

Full Screen / Esc

Printer-friendly Version

Interactive Discussion

keep a required distance of about 1.5 km to the cloud top to avoid overload of the detectors and data acquisition and maintain sufficient sensitivity at the same time. Comparisons with in-situ measurements of humidity on the research aircraft Falcon flying inside the cirrus cloud confirmed the high accuracy of the WALES system. The presented study shows the advantages of lidar cross-sections to provide additional information about the vertical structure of the humidity field compared to in-situ measurements. The profile data allow performing simultaneous statistical analysis in different cloud layers.

Since the Techno-Mission was focused mainly on the technical performance of aircraft and instruments, it is beyond the scope of this study to address all details of cirrus cloud formation to its full extent. The flights were limited with respect to the operation area and to local meteorological conditions. For the future, additionally data is required during the entire life cycle of a cirrus cloud. Future HALO missions, especially the ML-Cirrus mission, are focusing on this topic and will benefit from the findings and techniques presented in this article. The measurement of temperature profiles with a microwave temperature profiler, as planned for the ML-Cirrus mission, will allow elaborating the presented methods.

*Acknowledgements.* This work has been funded by the Deutsche Forschungsgemeinschaft (DFG) in the SPP (No. 1294/2) “Atmosphären- und Erdsystemforschung mit dem Forschungsflugzeug HALO (High Altitude and Long Range Research Aircraft)” under contract Nr. KI1567/1-1 and Nr. VO1504/2-1. S. Kaufmann was funded by the Helmholtz-Gemeinschaft Deutscher Forschungszentren e.V. (HGF) under contract VH-NG-309 within the Helmholtz-Hochschul Young investigators group AEROTROP. The authors like to thank the staff members of the DLR Falcon and the HALO aircraft from DLR Flight Experiments for preparing and performing the measurement flights and providing Falcon in-situ temperature measurements and analysis.

The service charges for this open access publication have been covered by a Research Centre of the Helmholtz Association.

## References

- Bösenberg, J.: Ground-based differential absorption lidar for water-vapor and temperature profiling: methodology, *Appl. Optics*, 37, 3845–3860, doi:10.1364/AO.37.003845, 1998.
- Chen, T., Rossow, W. B., and Zhang, Y.: Radiative effects of cloud-type variations, *J. Climate*, 13, 264–286, doi:10.1175/1520-0442(2000)013<0264:REOCTV>2.0.CO;2, 2000.
- Comstock, J. M., Ackerman, T. P., and Turner, D. D.: Evidence of high ice supersaturation in cirrus clouds using ARM Raman lidar measurements, *Geophys. Res. Lett.*, 31, L11106, doi:10.1029/2004GL019705, 2004.
- Cox, S. K.: Cirrus clouds and the climate, *J. Atmos. Sci.*, 28, 1513–1515, doi:10.1175/1520-0469(1971)028<1513:CCATC>2.0.CO;2, 1971.
- DeMott, P. J., Rogers, D. C., Kreidenweis, S. M., Chen, Y., Twohy, C. H., Baumgardner, D., Heymsfield, A. J., and Chan, K. R.: The role of heterogeneous freezing nucleation in upper tropospheric clouds: inferences from SUCCESS, *Geophys. Res. Lett.*, 25, 1387–1390, doi:10.1029/97GL03779, 1998.
- Ehret, G., Kiemle, C., Renger, W., and Simmet, G.: Airborne remote sensing of tropospheric water vapor with a near-infrared differential absorption lidar system, *Appl. Optics*, 32, 4534–4551, doi:10.1364/AO.32.004534, 1993.
- Esselborn, M., Wirth, M., Fix, A., Tesche, M., and Ehret, G.: Airborne high spectral resolution lidar for measuring aerosol extinction and backscatter coefficients, *Appl. Optics*, 47, 346–358, doi:10.1364/AO.47.000346, 2008.
- Fricke, C., Ehrlich, A., Jäkel, E., Bohn, B., Wirth, M., and Wendisch, M.: Influence of surface albedo heterogeneity on passive remote sensing of cirrus properties, *Atmos. Chem. Phys. Discuss.*, 13, 3783–3816, doi:10.5194/acpd-13-3783-2013, 2013.
- Fusina, F., Spichtinger, P., and Lohmann, U.: Impact of ice supersaturated regions and thin cirrus on radiation in the midlatitudes, *J. Geophys. Res.*, 112, D24S14, doi:10.1029/2007JD008449, 2007.
- Goff, J. A. and Gratch, S.: Low-pressure properties of water from –160 to 212° F, *Heat. Vent. Engrs.*, 52, 95–122, 1946.
- Gu, Y. and Liou, K. N.: Interactions of radiation, microphysics, and turbulence in the evolution of cirrus clouds, *J. Atmos. Sci.*, 57, 2463–2479, doi:10.1175/1520-0469(2000)057<2463:IORMAT>2.0.CO;2, 2000.

## Potential of airborne lidar measurements for cirrus cloud studies

S. Groß et al.

Title Page

Abstract

Introduction

Conclusions

References

Tables

Figures

◀

▶

◀

▶

Back

Close

Full Screen / Esc

Printer-friendly Version

Interactive Discussion



## Potential of airborne lidar measurements for cirrus cloud studies

S. Groß et al.

Title Page

Abstract

Introduction

Conclusions

References

Tables

Figures

◀

▶

◀

▶

Back

Close

Full Screen / Esc

Printer-friendly Version

Interactive Discussion



- Haag, W. and Kärcher, B.: The impact of aerosols and gravity waves on cirrus clouds at midlatitudes, *J. Geophys. Res.*, 109, D12202, doi:10.1029/2004JD004579, 2004.
- Haag, W., Kärcher, B., Ström, J., Minikin, A., Lohmann, U., Ovarlez, J., and Stohl, A.: Freezing thresholds and cirrus cloud formation mechanisms inferred from in situ measurements of relative humidity, *Atmos. Chem. Phys.*, 3, 1791–1806, doi:10.5194/acp-3-1791-2003, 2003.
- Heymsfield, A. J.: Precipitation development in stratiform ice clouds: a microphysical and dynamical study, *J. Atmos. Sci.*, 34, 367–381, doi:10.1175/1520-0469(1977)034<0367:PDISIC>2.0.CO;2, 1977.
- Heymsfield, A. J. and Miloshevich, L. M.: Relative humidity and temperature influences on cirrus formation and evolution: Observations from wave clouds and FIRE II, *J. Atmos. Sci.*, 52, 4302–4326, doi:10.1175/1520-0469(1995)052<4302:RHATIO>2.0.CO;2, 1995.
- IPCC: Climate Change 2007: the Scientific Basis, Cambridge University Press, 2007.
- IPCC: Climate Change 2013: The Physical Science Basis, Cambridge University Press, 2013.
- Kärcher, B.: Atmospheric ice formation processes, *Atmospheric Physics*, edited by: Schumann, U., *Research Topics in Aerospace*, Springer-Verlag, Berlin Heidelberg, 151–168, 2012.
- Kaufmann, S., Voigt, C., Jeßberger, P., Jurkat, T., Schlager, H., Schwarzenboeck, A., Klingebiel, M., and Thornberry, T.: In situ measurements of ice saturation in young contrails, *Geophys. Res. Lett.*, 41, 702–709, doi:10.1002/2013GL058276, 2014.
- Khvorostyanov, V. I. and Sassen, K.: Cirrus cloud simulation using explicit microphysics and radiation, Part I: Model description, *J. Atmos. Sci.*, 55, 18081821, doi:10.1175/1520-0469(1998)055<1808:CCSUEM>2.0.CO;2, 1998a.
- Khvorostyanov, V. I. and Sassen, K.: Cirrus cloud simulation using explicit microphysics and radiation; Part II: Microphysics, vapor and ice mass budgets, and optical and radiative properties, *J. Atmos. Sci.*, 55, 1822–1845, 1998b.
- Kiemle, C., Wirth, M., Fix, A., Ehret, G., Schumann, U., Gardiner, T., Schiller, C., Sitnikov, N., and Stiller, G.: First airborne water vapor lidar measurements in the tropical upper troposphere and mid-latitudes lower stratosphere: accuracy evaluation and intercomparisons with other instruments, *Atmos. Chem. Phys.*, 8, 5245–5261, doi:10.5194/acp-8-5245-2008, 2008.
- Koop, T., Luo, B., Tsias, A., and Peter, T.: Water activity as the determinant for homogenous ice nucleation in aqueous solutions, *Nature*, 406, 611–614, 2000.

## Potential of airborne lidar measurements for cirrus cloud studies

S. Groß et al.

Title Page

Abstract

Introduction

Conclusions

References

Tables

Figures

◀

▶

◀

▶

Back

Close

Full Screen / Esc

Printer-friendly Version

Interactive Discussion



Krautstrunk, M. and Giez, A.: The transition from Falcon to HALO era airborne atmospheric research, in: *Atmospheric Physics*, edited by: Schumann, U., *Research Topics in Aerospace*, 609–624, Springer, Berlin, Heidelberg, 2012.

Krebsbach, M., Koppmann, R., Bühler, F., Heuser, H.-P., Knieling, P., Scheidt, M., and Spahn, H.: Measurements of Stable Carbon Isotope Ratios in Atmospheric VOC on HALO during TACTS and ESMVal, EGU General Assembly 2013, held 7–12 April 2013 in Vienna, Austria, id. EGU2013-3853, 2013.

Liou, K.-N.: Light scattering by ice clouds in the visible and infrared: a theoretical study, *J. Atmos. Sci.*, 29, 524–536, 1972.

Liou, K.-N.: Influence of cirrus clouds on weather and climate processes: a global perspective, *Mon. Weather Rev.*, 114, 11671199, doi:10.1175/1520-0493(1986)114<1167:IOCCOW>2.0.CO;2, 1986.

Nash, J., Oakley, T., Vömel, H., and Wei, L. I.: WMO intercomparison of high quality radiosonde systems: Yanjiang, China, 12 July–3 August 2010, IOM Rep. 107, WMO/TD-1580, 238 pp., 2011.

Ovarlez, J., Gayet, J.-F., Gierens, K., Ström, J., Ovarlez, H., Auriol, F., Busen, R., and Schumann, U.: Water vapor measurements inside cirrus clouds in Northern and Southern Hemispheres during INCA, *Geophys. Res. Lett.*, 29, 1813, doi:10.1029/2001GL014440, 2002.

Roiger, A., Aufmhoff, H., Stock, P., Arnold, F., and Schlager, H.: An aircraft-borne chemical ionization – ion trap mass spectrometer (CI-ITMS) for fast PAN and PPN measurements, *Atmos. Meas. Tech.*, 4, 173–188, doi:10.5194/amt-4-173-2011, 2011.

Schäfler, A., Dörnbrack, A., Kiemle, C., Rahm, S., and Wirth, M.: Tropospheric water vapor transport as determined from airborne lidar measurements, *J. Atmos. Ocean. Tech.*, 27, 20172030, doi:10.1175/2010JTECHA1418.1, 2010.

Seifert, M., Ström, J., Krejci, R., Minikin, A., Petzold, A., Gayet, J.-F., Schlager, H., Ziereis, H., Schumann, U., and Ovarlez, J.: Aerosol-cirrus interactions: a number based phenomenon at all?, *Atmos. Chem. Phys.*, 4, 293–305, doi:10.5194/acp-4-293-2004, 2004.

Spichtinger, P., Gierens, K., Smit, H. G. J., Ovarlez, J., and Gayet, J.-F.: On the distribution of relative humidity in cirrus clouds, *Atmos. Chem. Phys.*, 4, 639–647, doi:10.5194/acp-4-639-2004, 2004.

Stefanutti, L., Sokolov, L., Balestri, S., MacKenzie, A. R., and Khattatov, V.: The M-55 geophysics as a platform for the airborne polar experiment, *J. Atmos. Ocean. Tech.*, 16, 13031312, doi:10.1175/1520-0426(1999)016<1303:TMGAAP>2.0.CO;2, 1999.

**Potential of airborne lidar measurements for cirrus cloud studies**

S. Groß et al.

[Title Page](#)[Abstract](#)[Introduction](#)[Conclusions](#)[References](#)[Tables](#)[Figures](#)[◀](#)[▶](#)[◀](#)[▶](#)[Back](#)[Close](#)[Full Screen / Esc](#)[Printer-friendly Version](#)[Interactive Discussion](#)

Stephens, G. L., Tsay, S.-C., Stackhouse Jr., P. W., and Flatau, P. J.: The relevance of the microphysical and radiative properties of cirrus clouds to climate and climatic feedback., J. Atmos. Sci., 47, 1742–1754, 1990.

5 Stickney, T. M., Shedlov, M. W., and Thompson, D. I.: Goodrich total temperature sensors, Technical Report 5755, Rosemount Aerospace Inc., Rev. C, 1994.

Voigt, C., Jeßberger, P., Jurkat, T., Kaufmann, S., Baumann, R., Schlager, H., Bobrowski, N., Guffirda, G., and Salerno, G.: Evolution of SO<sub>2</sub>, HCl, HNO<sub>3</sub> and CO<sub>2</sub> in the volcanic plume from Etna, Geophys. Res. Lett., in review, 2014.

10 Wirth, M., Fix, A., Mahnke, P., Schwarzer, H., Schrandt, F., and Ehret, G.: The airborne multi-wavelength h<sub>2</sub>o-dial wales: system design and performance, Appl. Phys. B, 96, 201–213, doi:10.1007/s00340-009-3365-7, 2009.

## Potential of airborne lidar measurements for cirrus cloud studies

S. Groß et al.

Title Page

Abstract

Introduction

Conclusions

References

Tables

Figures

⏪

⏩

◀

▶

Back

Close

Full Screen / Esc

Printer-friendly Version

Interactive Discussion



**Table 1.** Technical features of Gulfstream G550 HALO aircraft adopted from Krautstrunk and Giez (2012).

Engine	Rolls Royce BR710
Aircraft Performance	
Maximum range	12 500 km
Maximum cruise altitude	15 540 m
Take-off distance	1801 m
Maximum speed	0.885 Mach
Weights	
Maximum take-off weight	41 277 kg
Maximum payload	3 t
Exterior	
Length	29.4 m
Height	7.9 m
Wingspan	28.5 m
Interior	
Cabin length	15.3 m
Cabin height	1.88 m
Cabin width	2.24 m
Cabin volume	47.3 m <sup>3</sup>

## Potential of airborne lidar measurements for cirrus cloud studies

S. Groß et al.

Title Page

Abstract

Introduction

Conclusions

References

Tables

Figures

◀

▶

◀

▶

Back

Close

Full Screen / Esc

Printer-friendly Version

Interactive Discussion

**Table 2.** System parameters of WALES.

Transmitter type	Nd:YAG laser pumped OPO
Pulse energy (mJ)	40
Pulse rate (Hz)	200
Wavelength (nm)	532, 935, 1064
Strong absorbing line (nm)	935.6846
Medium absorbing line (nm)	935.6083
Weak absorbing line (nm)	935.5612
Telescope diameter (cm)	48
Vertical resolution (m)	150
Horizontal resolution (km)	1 (5 s)

## Potential of airborne lidar measurements for cirrus cloud studies

S. Groß et al.

**Table 3.** Mean values and relative variability (averaged between 11:25 and 11:54 UTC) along Falcon flight path on 4 Nov 2010. For the ECMWF relative humidity uncorrected model temperature data are used. In-situ relative humidity is determined from WARAN water vapour measurements and in-situ temperature measurements onboard the Falcon.

	Mean		Variability	
	ECMWF	In-situ	ECMWF	In-situ
Temperature/K	219	220	0.0003	0.0006
H <sub>2</sub> O mix/ppmv	100	99	0.03	0.12
RHi/%	103	91	0.03	0.12

[Title Page](#)
[Abstract](#)
[Introduction](#)
[Conclusions](#)
[References](#)
[Tables](#)
[Figures](#)
[⏪](#)
[⏩](#)
[◀](#)
[▶](#)
[Back](#)
[Close](#)
[Full Screen / Esc](#)
[Printer-friendly Version](#)
[Interactive Discussion](#)

# AMTD

7, 4033–4066, 2014

## Potential of airborne lidar measurements for cirrus cloud studies

S. Groß et al.



**Fig. 1.** HALO (High Altitude and Long range) aircraft. Photo adopted from <http://www.halo.dlr.de/>.

Title Page

Abstract

Introduction

Conclusions

References

Tables

Figures

⏪

⏩

◀

▶

Back

Close

Full Screen / Esc

Printer-friendly Version

Interactive Discussion



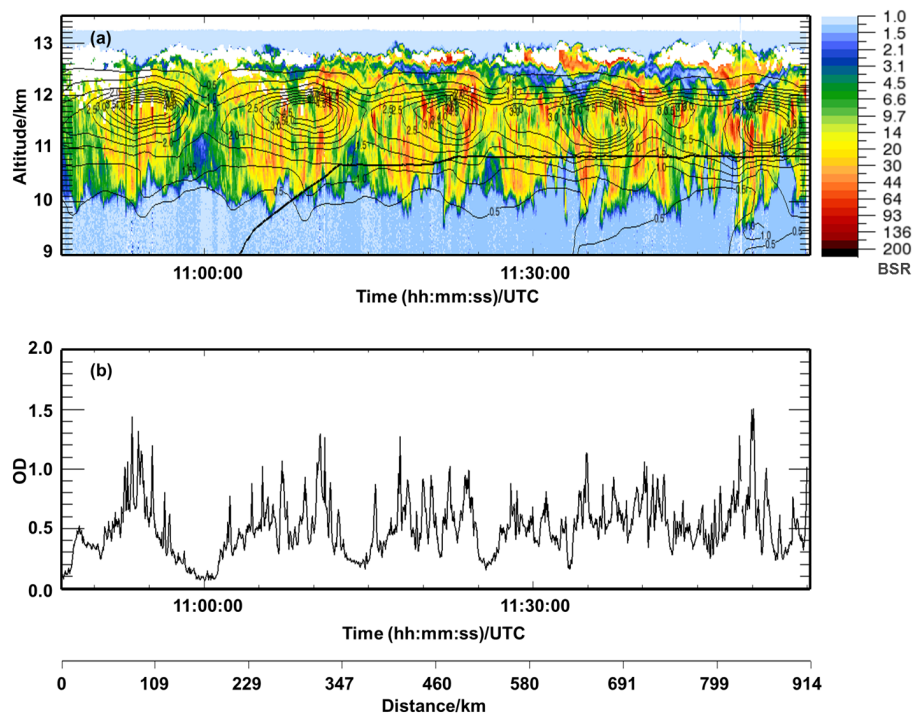


**Fig. 3. (a)** Backscatter ratio at 532 nm (colour shading) between 10:47 and 11:54 UTC on 4 November 2010. White areas are caused by signal overload. The thick black solid line indicates the altitude of the DLR Falcon; the black contour lines show the ECMWF cloud ice water content of 0.5–4.5 mg kg<sup>-1</sup>. **(b)** Optical depth (OD) at 532 nm of the cirrus cloud derived from WALES measurements.

## Potential of airborne lidar measurements for cirrus cloud studies

S. Groß et al.

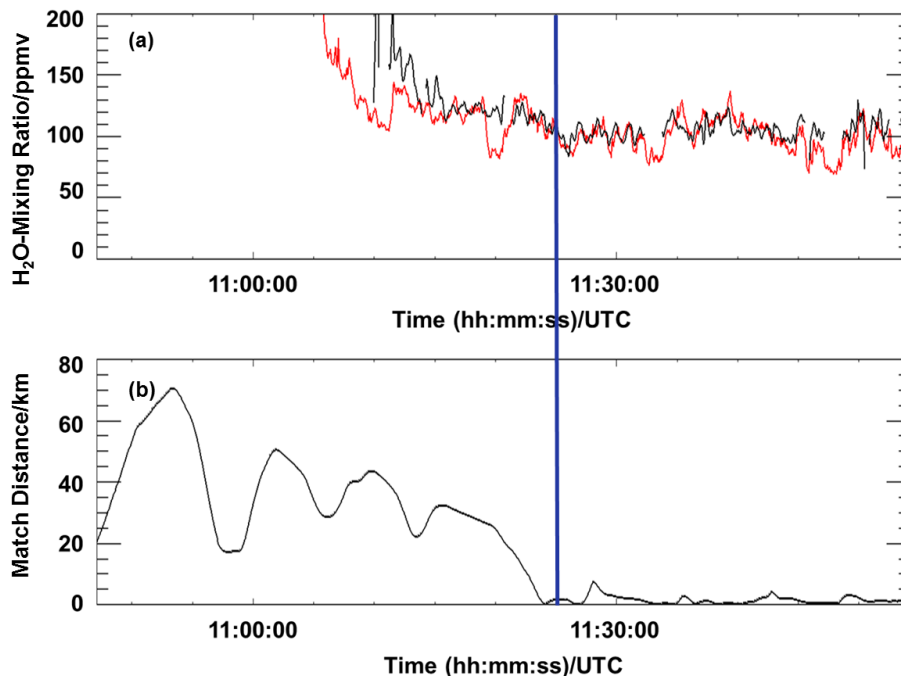


**Fig. 4.** (a) Water vapour mixing ratio as retrieved by the WARAN instrument flown on the Falcon (red line) and the WALES instrument (black line) at the same altitude. (b) Horizontal distance between the two aircraft as a function of time.

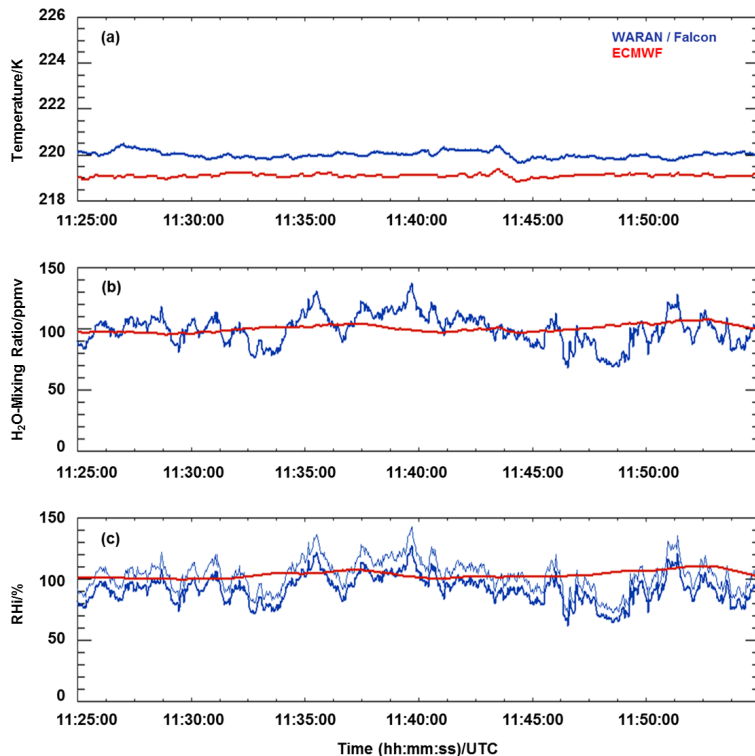


**Fig. 5.** Comparison of in-situ temperature, water vapour and RHi measurements on 4 November 2010 from WARAN onboard the Falcon (blue lines) with data from ECMWF model analysis (red lines). **(a)** Static air temperature, **(b)** water vapour mixing ratio and **(c)** relative humidity over ice along the flight track. The red line shows RHi calculated from ECMWF temperature and water vapour data, the thick blue line shows RHi calculated from WARAN water vapour mixing ratio and Falcon in-situ temperature measurements, and the thin blue line shows RHi calculated from WARAN water vapour mixing ratio measurements and ECMWF model temperature.

Potential of airborne lidar measurements for cirrus cloud studies

S. Groß et al.

Title Page

Abstract Introduction

Conclusions References

Tables Figures

⏪ ⏩

◀ ▶

Back Close

Full Screen / Esc

Printer-friendly Version

Interactive Discussion



## Potential of airborne lidar measurements for cirrus cloud studies

S. Groß et al.

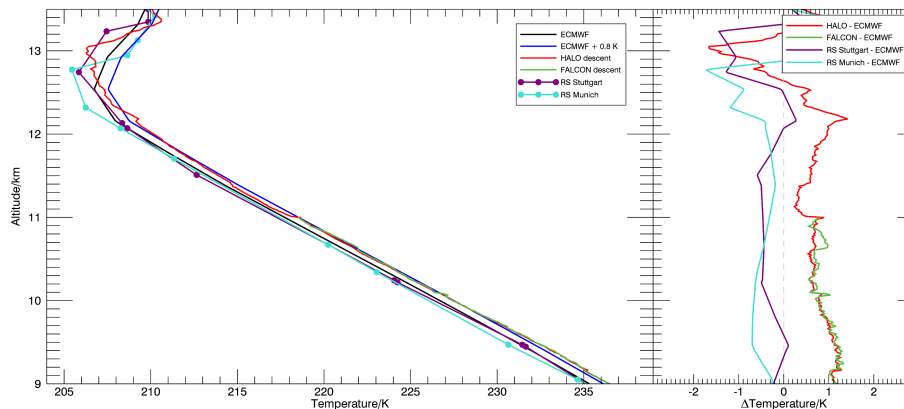


**Fig. 6.** (a) Temperature measurements from radiosondes over Munich (light blue line) and Stuttgart (purple line) at 12:00 UTC, 4 November 2010, ECMWF model analysis (black line) and in-situ measurements from HALO (red line) and Falcon (green line) descends. (b) Difference of ECMWF model analysis temperature data and HALO in-situ temperature measurements (red line), Falcon in-situ measurements (green line) during descends, and radiosonde temperature measurements over Munich (light blue line) and Stuttgart (purple line).

Title Page

Abstract

Introduction

Conclusions

References

Tables

Figures

◀

▶

◀

▶

Back

Close

Full Screen / Esc

Printer-friendly Version

Interactive Discussion

## Potential of airborne lidar measurements for cirrus cloud studies

S. Groß et al.

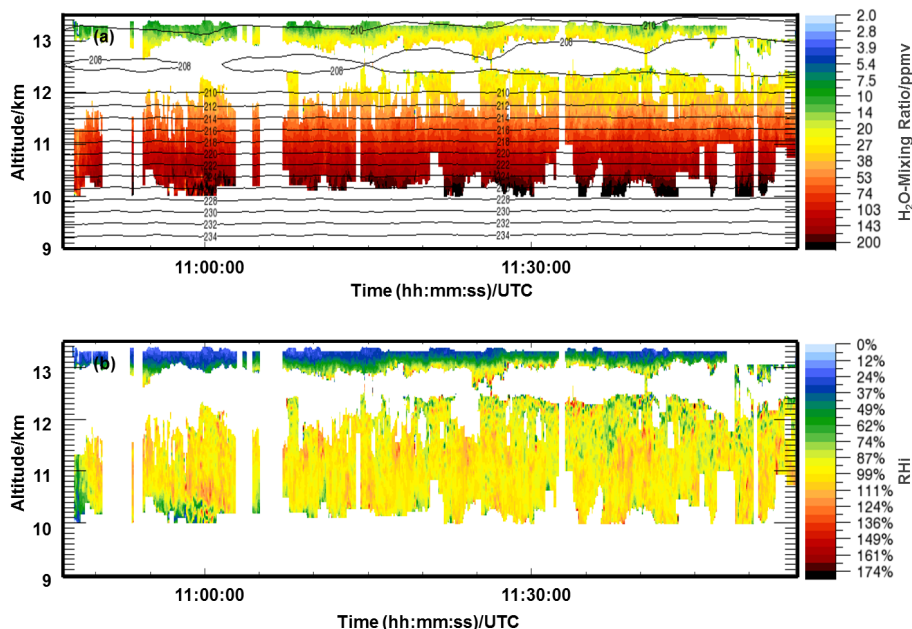


**Fig. 7.** (a) Water vapour volume mixing ratio as measured with WALES on HALO and contour lines of ECMWF temperature. (b) Relative humidity over ice from combined WALES and ECMWF data. In the white areas no trustworthy measurements are available due to signal overload and strong variability.

Title Page

Abstract

Introduction

Conclusions

References

Tables

Figures

◀

▶

◀

▶

Back

Close

Full Screen / Esc

Printer-friendly Version

Interactive Discussion

## Potential of airborne lidar measurements for cirrus cloud studies

S. Groß et al.

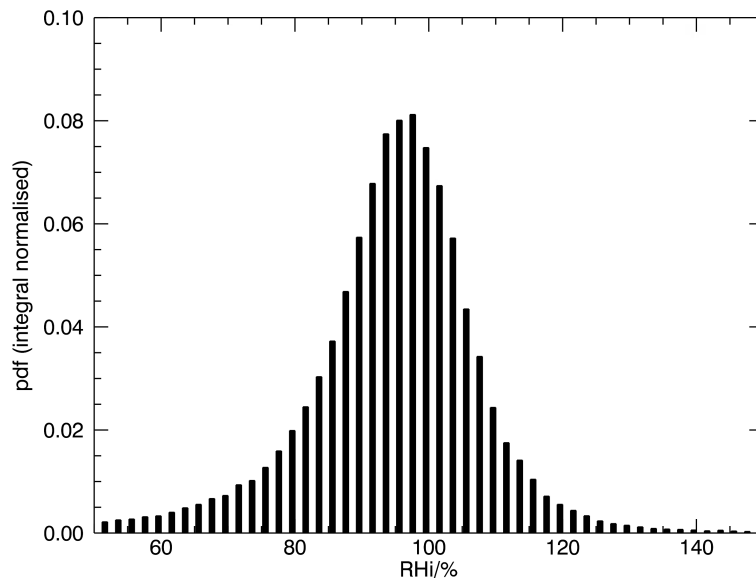


**Fig. 8.** Frequency distribution of the relative humidity over ice inside the cirrus cloud shown in Figs. 3 and 7. The bin size of the histogram is 2%.

[Title Page](#)[Abstract](#)[Introduction](#)[Conclusions](#)[References](#)[Tables](#)[Figures](#)[⏪](#)[⏩](#)[◀](#)[▶](#)[Back](#)[Close](#)[Full Screen / Esc](#)[Printer-friendly Version](#)[Interactive Discussion](#)

## Potential of airborne lidar measurements for cirrus cloud studies

S. Groß et al.

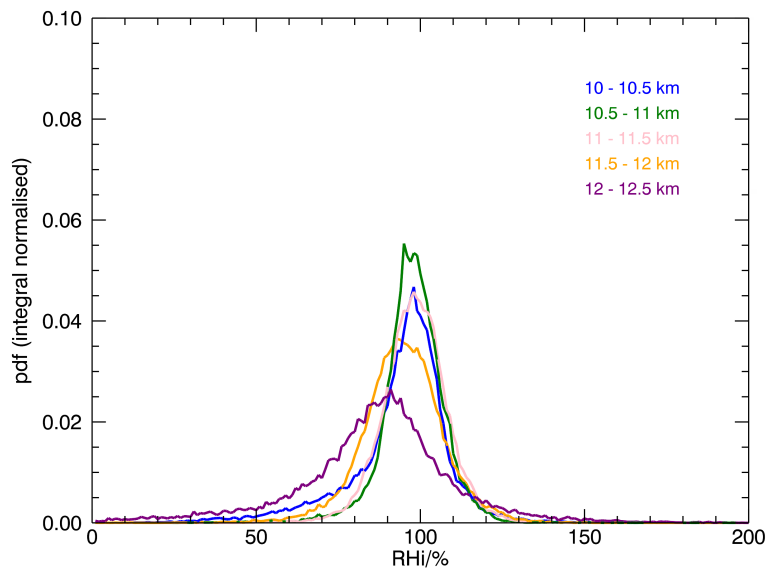


**Fig. 9.** Frequency distribution of the relative humidity over ice at different vertical layers inside the cirrus cloud shown in Figs. 3 and 7.

[Title Page](#)[Abstract](#)[Introduction](#)[Conclusions](#)[References](#)[Tables](#)[Figures](#)[◀](#)[▶](#)[◀](#)[▶](#)[Back](#)[Close](#)[Full Screen / Esc](#)[Printer-friendly Version](#)[Interactive Discussion](#)

